© 2018. Published by The Company of Biologists Ltd | Journal of Cell Science (2018) 131, jcs211631. doi:10.1242/jcs.211631

RESEARCH ARTICLE

TFIIH localization is highly dynamic during zygotic genome activation in *Drosophila*, and its depletion causes catastrophic mitosis

Grisel Cruz-Becerra, Sarai Valerio-Cabrera, Mandy Juárez, Alyeri Bucio-Mendez and Mario Zurita*

ABSTRACT

In *Drosophila*, zygotic genome activation occurs in pre-blastoderm embryos during rapid mitotic divisions. How the transcription machinery is coordinated to achieve this goal in a very brief time span is still poorly understood. Transcription factor II H (TFIIH) is fundamental for transcription initiation by RNA polymerase II (RNAPII). Herein, we show the *in vivo* dynamics of TFIIH at the onset of transcription in *Drosophila* embryos. TFIIH shows an oscillatory behaviour between the nucleus and cytoplasm. TFIIH foci are observed from interphase to metaphase, and colocalize with those for RNAPII phosphorylated at serine 5 (RNAPIIS5P) at prophase, suggesting that transcription occurs during the first mitotic phases. Furthermore, embryos with defects in subunits of either the CAK or the core subcomplexes of TFIIH show catastrophic mitosis. Although, transcriptome analyses show altered expression of several maternal genes that participate in mitosis, the global level of RNAPIIS5P in TFIIH mutant embryos is similar to that in the wild type, therefore, a direct role for TFIIH in mitosis cannot be ruled out. These results provide important insights regarding the role of a basal transcription machinery component when the zygotic genome is activated.

KEY WORDS: Zygotic genome activation, ZGA, TFIIH, *Drosophila*, Transcription

INTRODUCTION

In many organisms, the initial stages of embryonic development are directed by the action of maternal products deposited in eggs during oogenesis. Maternal mRNAs encoding factors that are required for the first developmental stages are eventually degraded; simultaneously, the expression of zygotic genes occurs in transcriptional waves (Zurita et al., 2008; Lee et al., 2014). In *Drosophila*, after fertilization, the embryo is a syncytium in which the nucleus undergoes a series of rapid, synchronized mitotic divisions that consist of only S and M phases (Mazumdar and Mazumdar, 2002). It has been proposed that the first wave of zygotic transcription begins at nuclear cycle eight (NC8) (Pritchard and Schubiger, 1996; De Renzis et al., 2007); however, transcription of a few zygotic genes prior to NC7 was recently reported (Ali-Murthy et al., 2013). Therefore, the exact moment of zygotic transcription onset at pre-midblastula transition (pre-MBT) embryos is currently controversial. After NC10, mitotic cycles slow down, and by NC14, expression of most of the zygotic genome is activated at the midblastula transition (MBT; Farrell and O'Farrell, 2014).

In *Drosophila*, zygotic genome activation (ZGA) is mediated by the transcription factors vielfältig/Zelda and the GAGA factor (Staudt et al., 2006; Li et al., 2014; Blythe and Wieschaus, 2016) in coordination with components of the basal transcription machinery, that must be recruited to the promoters of genes expressed either at the pre-MBT or MBT (Satija and Bradley, 2012). At the pre-MBT, ∼100 genes are reportedly expressed (Lott et al., 2011), and a recent study detected unpaused RNA polymerase II (RNAPII) on the promoters of 77 genes during pre-MBT, probably because these genes must be transcribed in a very short time span (Chen et al., 2013). Therefore, analysis of the dynamic factors that activate transcription is fundamental to understanding the mechanism of ZGA.

A central component of basal transcription machinery is TFIIH, a multi-protein complex composed of core [XPB (Hay), XPD, p62 (Tfb1), p52 (Mrn), p44 (Ssl1), p34 (Tfb4) and p8 (Tfb5) subunits] and CAK (Cdk7, CycH and MAT1 subunits) subcomplexes. The core and CAK subcomplexes form the holo-TFIIH complex, which participates in transcription mediated by RNAPII (Zurita and Merino, 2003; Compe and Egly, 2012). The XPB and XPD subunits are DNA helicases/ATPases, while the XPB subunit is also a DNA translocase required for transcription initiation (Egly and Coin, 2011; Fishburn et al., 2015). Additionally, phosphorylation of serine residues 5 and 7 of the C-terminal domain (CTD) of the largest RNAPII subunit by Cdk7 is required for RNAPII promoter escape and recruitment of mRNA modification and processing factors during transcription elongation (Hsin and Manley, 2012). In addition, the TFIIH core subcomplex participates in the nucleotide excision DNA repair mechanism (Coin et al., 2007), while CAK participates in controlling the cell cycle as an activating kinase for cyclin-dependent kinase complexes (reviewed in Schachter and Fisher, 2013).

Furthermore, a transitory complex between the CAK and XPD subunits has also been identified (Aguilar-Fuentes et al., 2006; Abdulrahman et al., 2013). In accordance with this interaction, XPD reportedly regulates Cdk7 localization and negatively modulates its function during cell cycle regulation in *Drosophila* embryos (Chen et al., 2003; Li et al., 2010). However, XPD has been demonstrated to be a component of the MMXD complex, which is involved in chromosome segregation in human cells; thus, XPD depletion produces catastrophic mitosis (Ito et al., 2010). Furthermore, in *Drosophila*, XPD physically and genetically interacts with Galla, the fly homologue of a component of the human MMXD complex, which when defective also causes catastrophic mitosis during early embryonic nuclear division (Yeom et al., 2014).

Departamento de Genética del Desarrollo y Fisiología Molecular, Instituto de Biotecnología. Universidad Nacional Autónoma de México, Av Universidad 2001, Cuernavaca Morelos 62250, México.

*Author for correspondence (marioz@ibt.unam.mx)

S.V., 0000-0001-6676-8440; M.Z., 0000-0002-8404-2173

Received 3 October 2017; Accepted 3 April 2018

Journal of Cell Science (2018) 131, jcs211631. doi:10.1242/jcs.211631

Therefore, the general transcription factor TFIIH is involved in at least three fundamental cellular processes: transcription, DNA repair and cell cycle regulation. Although several studies have concentrated their efforts on the analysis of TFIIH functions *in vitro* and *in vivo*, fundamental questions remain to be answered, including whether mutations in other core subunits of TFIIH also affect mitosis, whether all TFIIH subunits have the same dynamics during early embryonic development, and how TFIIH subunits participate in zygotic gene activation. In this work, we have addressed these questions by analysing the *in vivo* dynamics of TFIIH subunits during early mitotic division cycles in fly embryos as well as the effect of the absence of TFIIH components on the syncytial blastoderm stage.

RESULTS

TFIIH shows highly dynamic behaviour at transcription onset in the syncytial blastoderm

We previously reported the localization of the XPB, XPD, Cdk7 and MAT1 TFIIH subunits during early *Drosophila* embryonic development (Aguilar-Fuentes et al., 2006). Using immunostaining analysis, we showed that during the early pre-blastoderm stage, XPB and XPD were preferentially cytoplasmic. At NC10 some XPB and XPD signals were detected inside the nucleus, while most Cdk7 and MAT1 remained cytoplasmic. Furthermore, chromatin immunoprecipitation (ChIP) experiments indicated that both core and CAK subunits could be found at some promoters at pre-MBT embryos (Aguilar-Fuentes et al., 2006). In contrast, a recent report using a different protocol for embryo immunostaining preparation revealed Cdk7 in the nucleus at the NC13 and NC14 interphases (Li et al., 2010).

Based on this information, we decided to refine our previous analysis of TFIIH dynamics during early embryonic development and determine the *in vivo* dynamics of TFIIH during fast mitotic cycles at the pre-MBT by performing immunostaining and via tagged fluorescent proteins. p8 is the smallest TFIIH subunit, and although it does not have enzymatic activity, it has been proposed to play an important role in the maintenance of steady-state TFIIH levels in human fibroblasts (Giglia-Mari et al., 2004). Initially, we studied the dynamics of this protein at pre-MBT embryos when ZGA takes place. Using immunostaining analysis and confocal microscopy, we found that at NC10 interphase, p8 was mostly nuclear. Furthermore, overlapping signals for p8 and chromosomes were observed (Fig. 1A). Intriguingly, at metaphase, most of the p8 signal was observed surrounding the chromosomes (Fig. 1B,C), and only slightly overlapped with the DNA and the mitotic spindle (Fig. 1D). In contrast, the p8 signal did not overlap with the nuclear envelope (which is not completely disassembled during syncytial blastoderm mitosis; Foe and Alberts, 1983; Harel et al., 1989), as

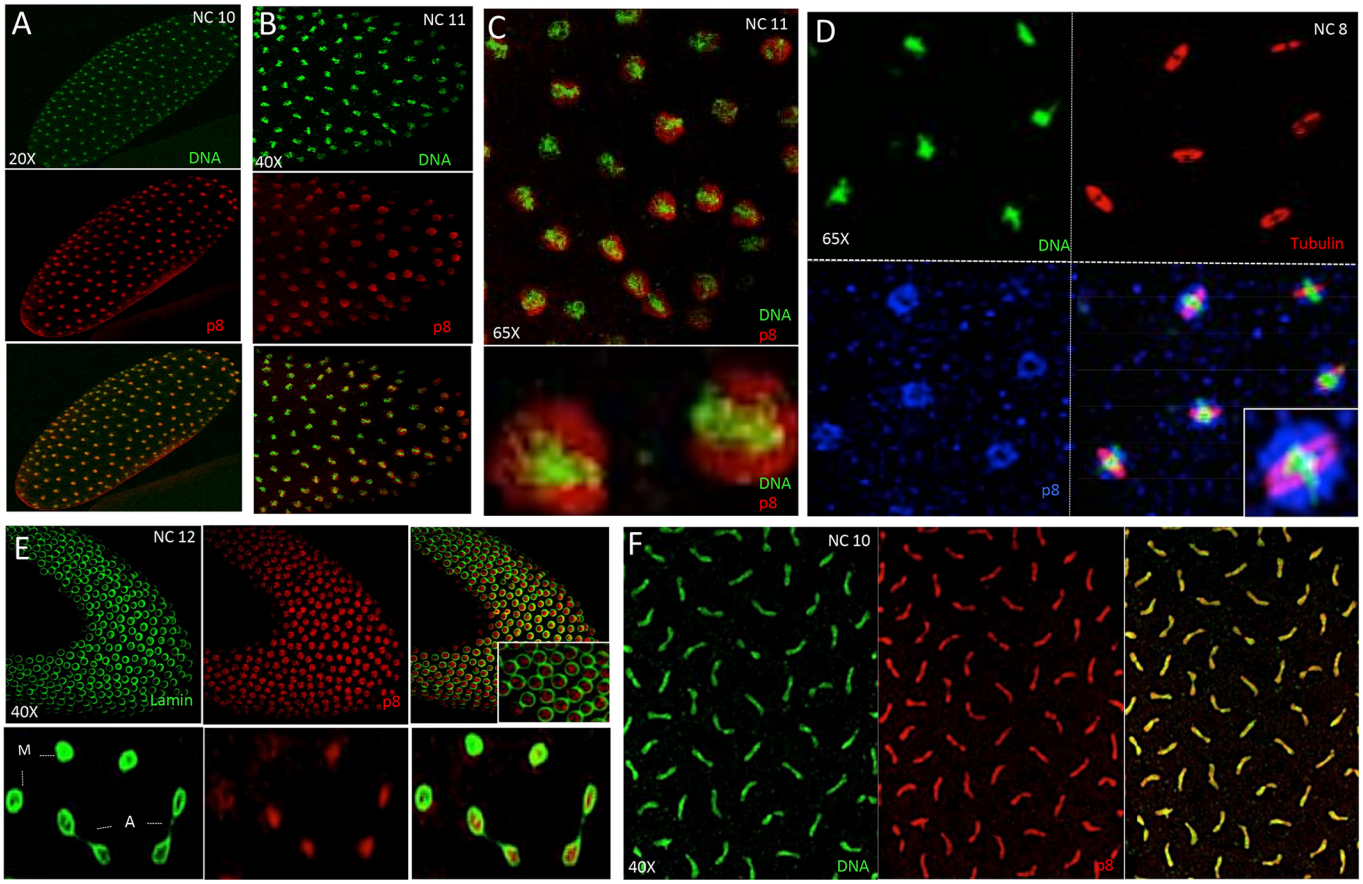

Fig. 1. p8 is preferentially nuclear during the mitotic cycles in the syncytial blastoderm embryo. (A) p8 is distributed in the nucleoplasm during interphase. (B,C) Most p8 (red) surrounds the chromosomes (green), although some p8 colocalizes with the chromosomes at metaphase. (D) At metaphase, p8 surrounds the mitotic structures, and also colocalizes with chromosomes and the mitotic spindle. p8, blue; β-tubulin, red; DNA, green. (E) Immunolocalization of lamin (green) and p8 (red) in syncytial blastoderm embryos at interphase (left) and mitosis (right) shows that p8 does not overlap with the nuclear membrane during the nuclear division cycle. M, metaphase; A, anaphase. (F) p8 (red) overlaps with chromosomes (green) at anaphase. All images correspond to projections of *z*-stacks acquired by confocal microscopy and the NC for each embryo is indicated in the figure. Magnifications relate to objective lens use.

Journal of Cell Science (2018) 131, jcs211631. doi:10.1242/jcs.211631

determined by anti-p8 and anti-Lamin co-immunostaining (Fig. 1E), indicating that most p8 at metaphase is maintained inside the nuclear lumen. In addition, the p8 signal still clearly overlapped with chromosomes at anaphase (Fig. 1F). This localization of p8 during mitosis has not been reported for any TFIIH subunits, suggesting that p8 could have different dynamics than those of other TFIIH components.

In the context of TFIIH, p8 physically interacts with p52, and this interaction has been reported to be important for TFIIH functions (Kainov et al., 2008; Cruz-Becerra et al., 2016). We therefore decided to analyse whether the dynamics of p52 were similar to those of p8 during syncytial blastoderm mitotic cycles. Although several very specific anti-p52 antibodies exist for western blot analysis (Villicaña et al., 2013), these do not work well for immunostaining. Therefore, we generated transgenic flies expressing recombinant p52 tagged with enhanced yellow fluorescent protein (EYFP). We previously reported that this EYFP–p52 construct could rescue several lethal *p52* alleles (Cruz-Becerra et al., 2016), suggesting that this fusion protein is functional. Furthermore, this result provides confidence that the dynamics of this protein observed *in vivo* are similar to those of the wild-type protein. To visualize the different mitotic cycle phases through chromatin dynamics, we took advantage of the previously reported transgenic line in which histone H2Av is fused to red fluorescent protein (H2Av–RFP) (Schuh et al., 2007). Fig. 2A (also see Movie 1 and Fig. S1) shows *z*-stacks projections of confocal images of an embryo expressing EYFP–p52 and H2Av–RFP. Although some signal was observed in the cytoplasm at the NC11 interphase, most EYFP–p52

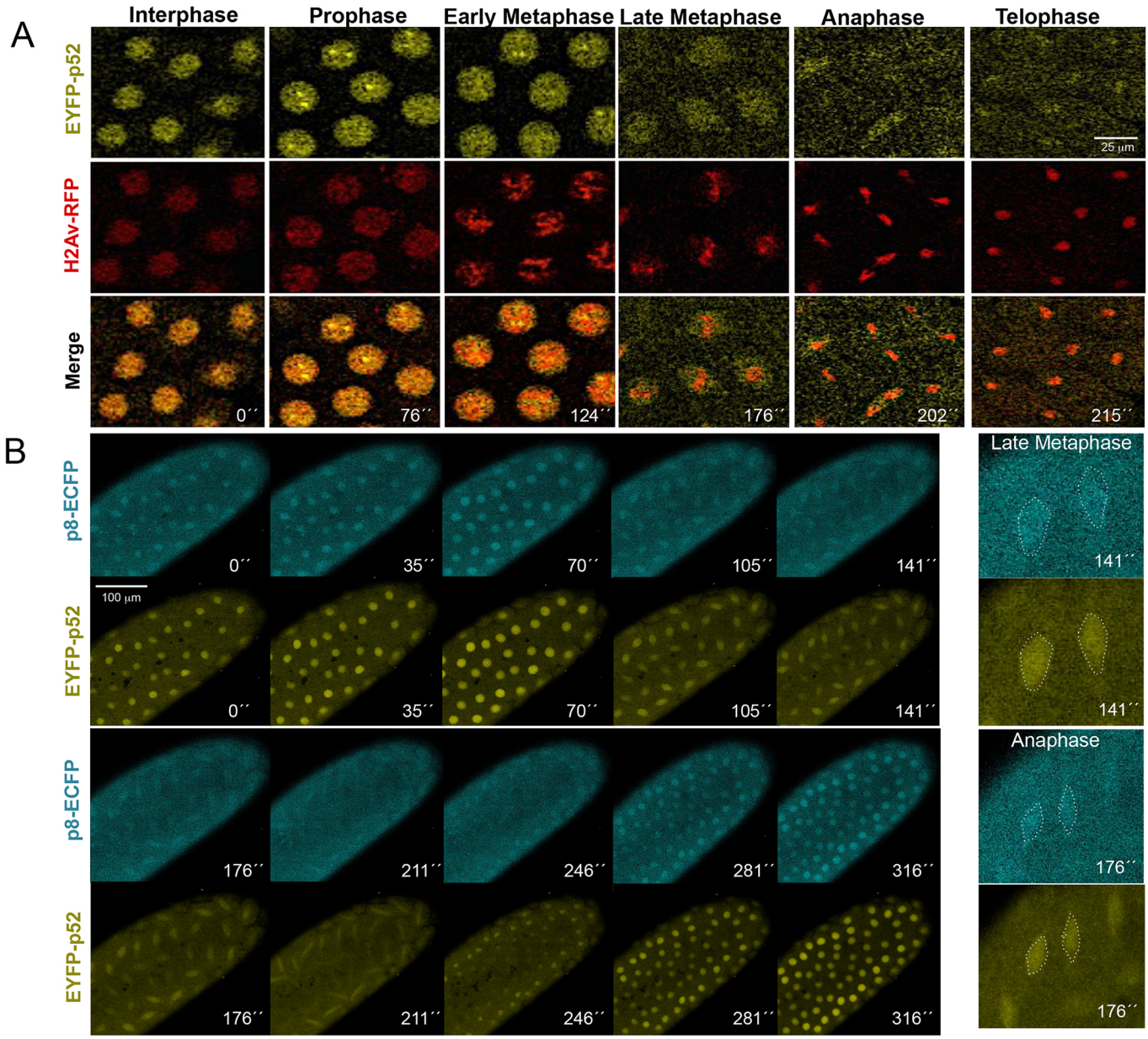

Fig. 2. The core and CAK TFIIH subunits follow similar dynamics during the syncytial blastoderm stage. (A) Visualization of an *EYFP-p52*/*H2Av-RFP* (yellow/red) transgenic pre-MBT embryo during a nuclear division cycle (the time in seconds is shown). The different stages of the mitotic cycle were identified using H2Av–RFP. Also see Movie 1. (B) Time-lapse analysis of a pre-MBT embryo expressing EYFP–p52 (yellow) and p8–ECFP (cyan) (also see Movies 2 and 3, and Fig. S1).

Journal of Cell Science (2018) 131, jcs211631. doi:10.1242/jcs.211631

signal overlapped with chromosomes, and intriguingly, EYFP–p52 nuclear foci were clearly observed (Fig. 2A; Movie 1). During early prophase, the EYFP–p52 signal was reduced in the cytoplasm and enriched in the nucleus. Furthermore, the number of EYFP–p52 nuclear foci was increased (in general, two to four foci per nucleus could be observed), and they were more evident at late prophase (Fig. 2A; Movie 1). The nuclear EYFP–p52 signal was reduced, but some EYFP–p52 surrounded chromosomes during metaphase and overlapped with the chromosomes at anaphase. While nuclear EYFP–p52 was significantly decreased at telophase, some EYFP–p52 overlap with the chromosomes was always detectable (Fig. 2A; Movie 1; Fig. S1).

Although the p8 chromosomal localization detected by immunostaining is clearest (Fig. 1), probably due to the tissue being fixed, the dynamic behaviour observed *in vivo* for EYFP–p52 was similar during NC8 to NC12 (Fig. 2), suggesting that these proteins follow the same dynamics in pre-MBT embryos. To confirm these results, we next analysed the dynamics of p8 *in vivo* using transgenic flies expressing recombinant p8 tagged with enhanced cyan fluorescent protein (ECFP). We have previously successfully demonstrated the functionality of the p8–ECFP recombinant protein by performing rescue experiments in a *p8*-null background (Cruz-Becerra et al., 2016). To directly compare the *in vivo* dynamics of p8 and p52, we generated flies that simultaneously expressed EYFP–p52 and p8–ECFP. Fig. 2B (see also Movie 2) shows the time-lapse sequence of one mitotic cycle in a pre-MBT embryo expressing both transgenes. We observed overlap in the signal of these proteins at all nuclear division stages, indicating highly similar dynamic oscillations between the nucleus and cytoplasm for these two components of the TFIIH core subcomplex. Specifically, the nuclear localization of p52 and p8 during mitosis, which has never been described for any TFIIH subunits in any organism, was intriguing.

The p52 subunit of TFIIH is essential for anchoring XPB to the complex (Jawhari et al., 2002); in addition, its role in modulating the ATPase activity of XPB has been extensively documented (Coin et al., 2007; Fregoso et al., 2007). Thus, we reasoned that if the TFIIH core is assembled during mitosis, XPB would behave similarly to p8 and p52. In our previous studies, we observed the exclusion of XPB from mitotic chromosomes in gastrulated embryos using an antibody against XPB (Aguilar-Fuentes et al., 2006). We therefore analysed the *in vivo* dynamics of fluorescently tagged XPB in syncytial blastoderm embryos, as was done for p8 and p52. XPB–EGFP or XPB–mCherry recombinant proteins follow dynamics along the mitotic cycle similar to those of p8 and p52 (Movie 3 and Fig. S2). Therefore, the *in vivo* results indicate that these core TFIIH subunits are retained in the nuclear lumen and suggest colocalization with the chromosomes during mitosis.

As mentioned previously, the holo-TFIIH complex (composed of the core and CAK subcomplexes) is required for transcription by RNAPII. Considering that ZGA occurs during the pre-MBT, we expected to observe core and CAK colocalization in transcriptionally active nuclei in pre-MBT embryos (i.e. at the interphase of NC8 and onwards). However, in addition to the nuclear localization of TFIIH core subunits during interphase, in this study, we noted some nuclear localization during mitosis in pre-MBT embryos (Figs 1 and 2). Thus, we considered the possibility of nuclear CAK localization during mitosis. To answer this question, we tested several antibodies against Cdk7, MAT1 and CycH for immunostaining in wild-type embryos (data not shown, Fig. S3). Intriguingly, CycH, a CAK component whose localization has not been analysed in pre-MBT embryos, showed similar dynamics to the core components of TFIIH described in this study. The CycH signal overlapped with chromosomes during mitosis, although a significant signal was detected in the cytoplasm, as expected (Fig. S3). Furthermore, we constructed flies that expressed a recombinant Cdk7–EGFP protein that showed the same dynamics as CycH and the core TFIIH subunits (Fig. S1; Movie 4). This indicates that at least part of both the core and CAK subunits remain in the nucleus during mitosis, and partially overlap with the mitotic chromosomes in pre-MBT embryos.

TFIIH foci are present throughout most of the syncytial blastoderm mitotic cycle and colocalize with active transcriptional foci

As indicated previously, EYFP–p52 was observed in granular structures in the nuclei of syncytial blastoderm embryos. These nuclear foci could also be visualized in transgenic embryos expressing XPB–mCherry and XPB–EGFP (Movie 3). The foci appeared simultaneously in nuclei at the anterior and posterior poles during interphase and were maintained until early metaphase (Fig. 3A,C). In addition, the foci located randomly in the nuclear lumen, with no specific apical or basal positioning. Interestingly, these EYFP–p52 foci did not overlap with the areas showing highest chromatin compaction (indicated by the low intensity of the H2Av-RFP nuclear signal in these regions) (Fig. 3A,C), suggesting that transcription could take place in these foci. Furthermore, it is known that in syncytial blastoderm nuclei, the form of RNAPII that is phosphorylated at serine 5 (RNAPIIS5P) is enriched in two foci (Seydoux and Dunn, 1997; Chen et al., 2013) that correspond to histone locus bodies (HLBs; these contain the histone genes that are organized in several tandem repeats, as well as factors required for histone mRNA synthesis; Salzler et al., 2013). Histone genes are transcribed at the S-phase during the pre-MBT (Nizami et al., 2010; Salzler et al., 2013); thus, these foci could be sites of TFIIH enrichment. Therefore, by assessing the dynamics of TFIIH foci in time-lapse experiments, we could potentially visualize spatial and temporal gene expression in pre-MBT stages. Immunostaining of EYFP–p52 early syncytial blastoderm embryos using an antibody against the RNAPIIS5P revealed that the signal of active RNAPII overlapped with some EYFP–p52 foci (Fig. 3B), suggesting that these nuclear structures are sites of basal transcription machinery recruitment for the zygotic transcription of the histone genes.

Interestingly, by following the same foci from interphase to late metaphase in the mitotic nuclei of syncytial blastoderm embryos (arrows in Fig. 3C) revealed that although histone genes are highly transcribed at S phase (Guglielmi et al., 2013), the TFIIH foci were maintained when mitosis was initiated, suggesting that transcription might overlap with the first stages of mitosis at the pre-MBT. Furthermore, for the p52 subunit of TFIIH, we observed three or four foci in some nuclei (Fig. 3A; Movies 1 and 3); however, the functions of the additional foci remain to be determined.

Essential role of TFIIH for proper mitosis in pre-MBT stages

The overlapping of the TFIIH signal with chromosomes at prophase, metaphase and anaphase suggests a possible role for TFIIH in mitosis in the pre-MBT embryo. The CAK TFIIH subcomplex plays an important role in controlling the cell cycle (reviewed in Schachter and Fisher, 2013); mutations in Cdk7 disrupt mitosis (Larochelle et al., 2007). Furthermore, depletion of XPD in *Drosophila* embryos reportedly causes mitotic defects by inducing Cdk7 localization on mitotic chromosomes (Lee et al., 2010). Nonetheless, a TFIIH-independent role for the XPD core subunit in

Journal of Cell Science (2018) 131, jcs211631. doi:10.1242/jcs.211631

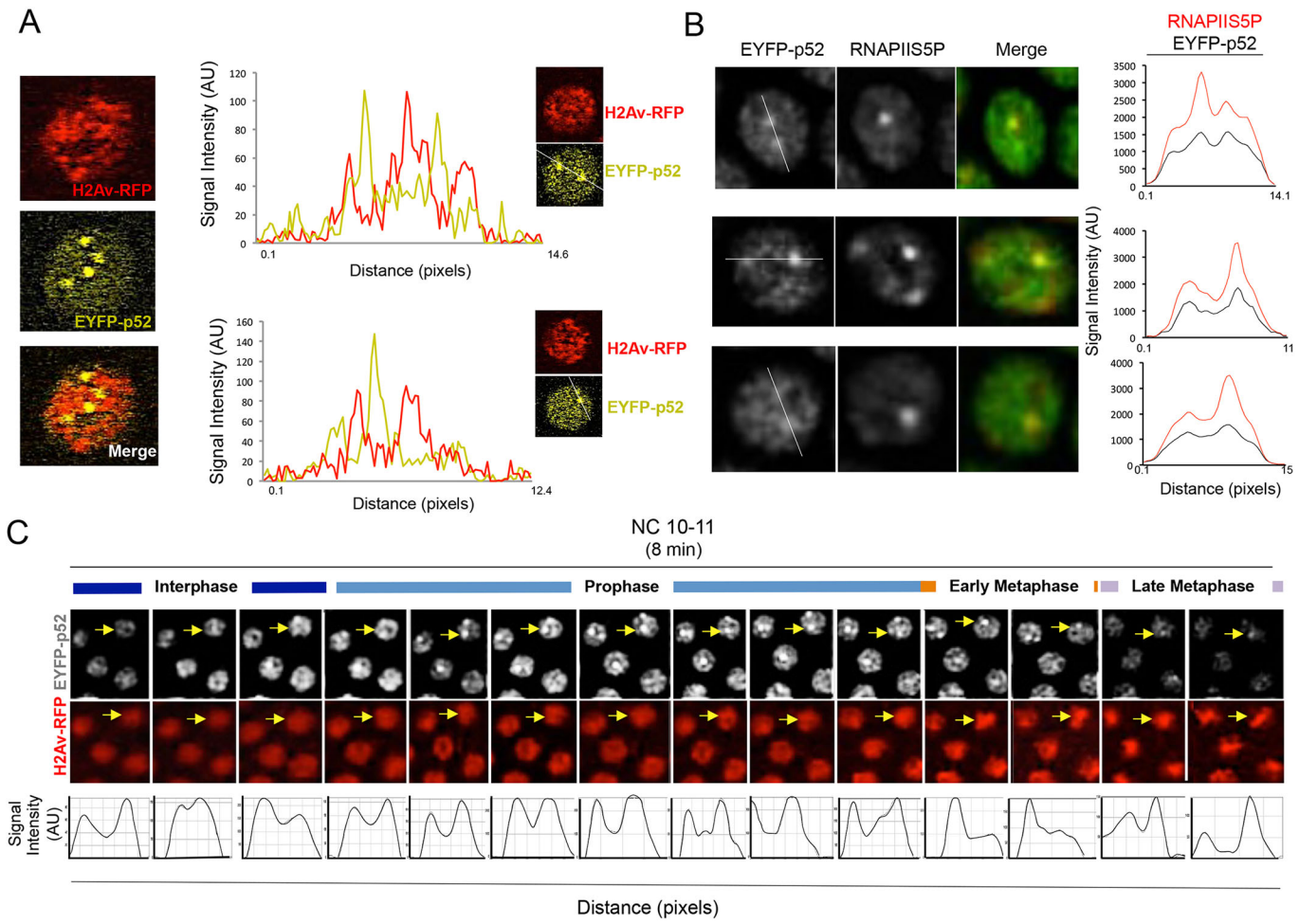

Fig. 3. TFIIH is enriched at transcribed chromatin in most of the mitotic cycle in the syncytial blastoderm. (A) Nuclei at interphase expressing EYFP–p52 (yellow) and H2Av–RFP (red) recombinant proteins in which TFIIH foci are observed. The plots are scans of both signals in a single confocal plane showing that regions of TFIIH enrichment are reduced in the H2Av–RFP signal. The lines on the nuclei indicate the scanning track. (B) RNAPII-enriched regions colocalize with TFIIH foci at the syncytial blastoderm. The plots show the location in a single plane of both signals for the line shown in the left panel. (C) Time-lapse analysis of TFIIH foci during a replicative cycle. TFIIH (EYFP–p52) foci (indicated by the arrows) were followed during a replicative cycle using the H2Av–RFP recombinant protein as a reference for stage. The time-lapse shows nuclei from the beginning of the interphase to metaphase in a syncytial blastoderm embryo between the NC10 and NC11 replicative cycles. The plots show the location in a single plane of the TFIIH foci. AU, arbitrary units.

chromosome segregation during mitosis has been suggested (Ito et al., 2010). However, whether core TFIIH subunits other than XPD participate in mitosis remains unknown. Thus, we analysed the effects of the absence of core TFIIH subunits on syncytial blastoderm embryos.

We recently characterized a *p8*-null allele that shows semi-lethality, as ∼25% of the expected homozygous organisms develop into adults. Of these adults, the males are sterile, and the females lay fewer eggs than wild-type flies (Herrera-Cruz et al., 2012). Importantly, the embryos laid by homozygous *p8*-null females do not have maternally deposited p8 and are thus an excellent tool to analyse the phenotypes produced by the absence of p8 in the early embryos. As shown in Fig. 4A, in homozygous *p8*-null females, although oogenesis could be completed, ∼90% of the egg chambers and laid eggs were smaller than wild type (Fig. 4C); this suggests transcriptional deficiencies during oogenesis, as we have previously observed in other organs with TFIIH loss of function (Fregoso et al., 2007; Villicaña et al., 2013). We next analysed the effect of the absence of p8 in early syncytial blastoderm embryos, which is when embryos are committed to nuclear division cycles. Intriguingly ∼20% of the embryos escape lethality and develop into adults without apparent phenotype. By staining microtubules and chromosomes in *p8*-null embryos, we observed failure to exit mitosis and mitotic catastrophes with different levels of severity in ∼60% of the embryos after NC8 (Fig. 4C–F; Fig. S4A). In *p8*-null nuclei at metaphase, the spindle was misaligned and longer than that in wild-type embryos; furthermore, some metaphase chromosomes were under-compacted (Fig. 4D), and isolated centrosomes and chromosomes were observed (Fig. 4D,E). During anaphase, the localization of histone H3 phosphorylated at serine 10 (H3S10P) was restricted to the telomeric region of the chromosomes in wild-type embryos, while in *p8*-null embryos, the localization of this mitotic marker was maintained throughout the chromosome bodies, even at telophase (Fig. 4F). All these defects in mitosis were supressed in *p8*-null embryos expressing the p8–ECFP recombinant protein (Cruz-Becerra et al., 2016).

Importantly, human cells derived from TTDA patients, affected in the human p8 gene (*GTF2H5*) have been shown to exhibit reduced levels of all other TFIIH subunits (Vermeulen et al., 2000; Giglia-Mari et al., 2004). However, we recently reported that the absence of p8 in *Drosophila* testes does not affect the levels of the other TFIIH subunits (Cruz-Becerra et al., 2016). To determine

Journal of Cell Science (2018) 131, jcs211631. doi:10.1242/jcs.211631

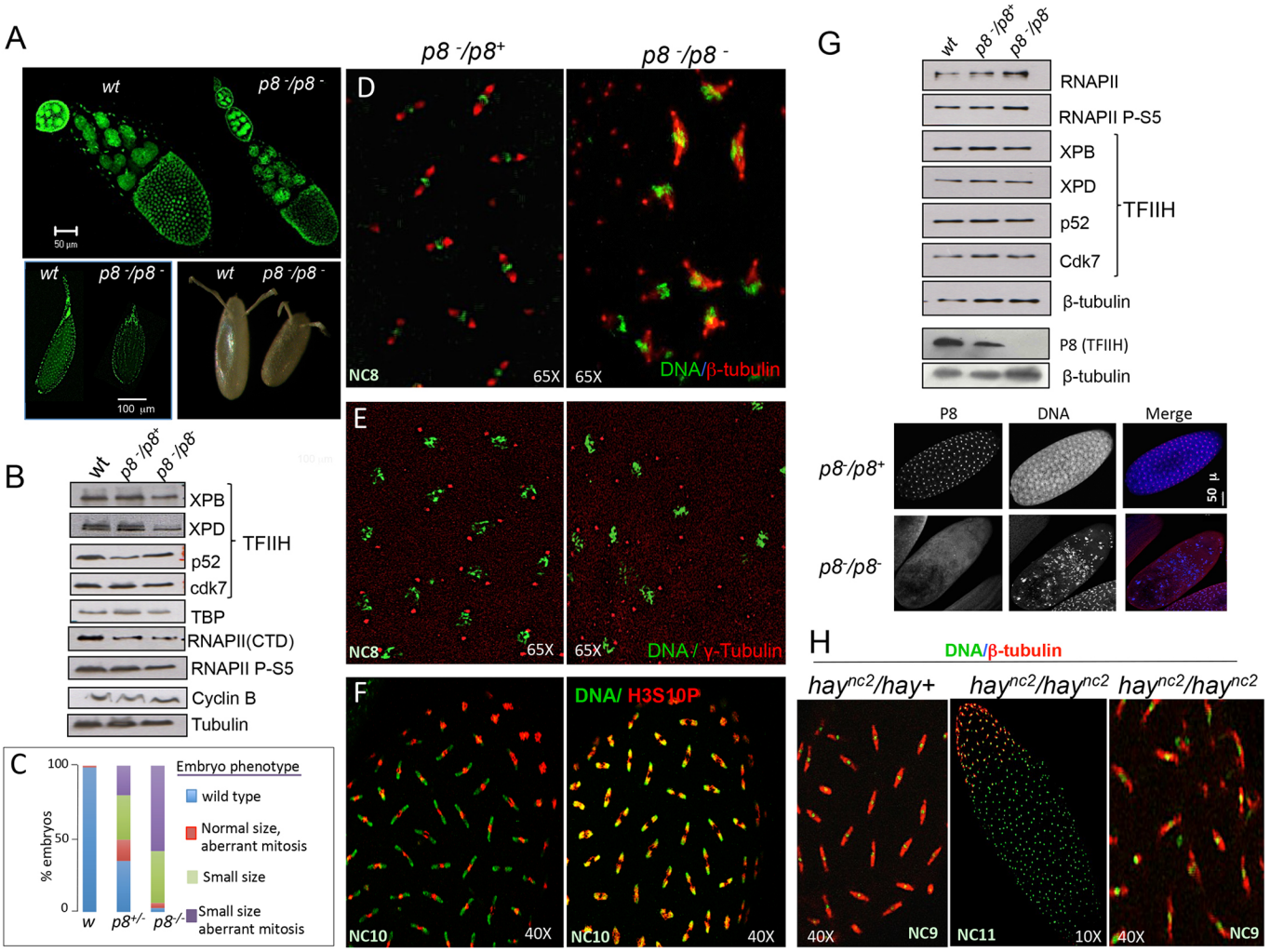

Fig. 4. The absence of functional TFIIH causes catastrophic mitosis in the syncytial blastoderm embryo. (A) Wild-type (wt) and *p8*-null ovaries, and the embryos laid, stained with SYTOX Green to visualize the DNA, from wild-type and *p8*-null mothers. (B) Western blot from total ovaries stained for proteins for different subunits of TFIIH, components of the basal transcription machinery and β-tubulin as loading control. (C) Penetrance of the small embryo and catastrophic mitosis phenotypes. (D) Comparison of mitosis between wild-type and *p8*-null embryos. The mitotic spindle was detected with an anti-β-tubulin antibody (red); DNA (green) was detected with SYTOX Green. (E) Detection of centrosomes in wild-type and *p8*-null embryos using a γ-tubulin antibody (red) and DNA (green) with SYTOX Green. (F) Alterations in mitosis cycle timing in *p8*-null embryos as compared to wild-type organisms as determined by visualizing the presence of H3 phosphorylated at serine 10 (H3S10P). (G) Upper panel: western blot from *p8*-null or wild-type embryos to determine the levels of different TFIIH subunits (including p8) and the RNAPII CTD phosphorylated at serine 5 (RNAPII P-S5). Lower panel: immunostainings of homozygous *p8*-null or *p8*-heterozygous embryos using the anti-p8 antibody. (H) Syncytial blastoderm embryos from heterozygous *hay*^{nc2} females and embryos from homozygous *hay*^{nc2} females stained with the anti-β-tubulin antibody and with SYTOX Green. A desynchronized embryo is presented in the middle, and an magnification showing catastrophic mitosis in a homozygous *hay*^{nc2} embryo is presented on the right. All the genotypes and antibodies used are indicated in the figure.

whether the catastrophic mitosis observed in syncytial blastoderm embryos lacking p8 could be an indirect effect of the deficiency of other TFIIH subunits, we analysed the levels of some core and CAK subunits in egg chambers and embryos from *p8*-null flies. Intriguingly, we did not find a significant reduction in the levels of the TFIIH components analysed, nor did we find changes in the levels of other transcription factors or RNAPIIS5P (Fig. 4G). Therefore, the mitotic catastrophes observed in *p8*-null embryos were only due to the absence of p8, suggesting that p8 might have a role in mitosis.

The question of whether mutations in TFIIH subunits other than p8 and XPD also affect mitosis in early embryos emerged. Thus, we analysed the XPB (*haywire* in fly) mutant allele *hay*^{nc2} (Mounkes et al., 1992; Merino et al., 2002). This allele is also semi-lethal, and homozygous females having this allele lay few fertilized eggs. Intriguingly, ∼60% of these embryos showed defects in mitosis, including free centrosomes, incompletely compacted chromosomes at metaphase and isolated chromosomes not attached to the mitotic spindle (Fig. 4F). On the other hand, less than 10% of the embryos from heterozygous *hay*^{nc2} females presented defects in mitosis. Because both XPB and p8 are core TFIIH subunits, analysing whether CAK loss of function also generates embryos with defects in mitosis was relevant. To achieve this, we constructed flies that expressed RNAi against the Cdk7 transcript during oogenesis, thereby generating embryos with reduced levels of this CAK component (Fig. S4B). These embryos showed mitotic defects, including aberrant mitotic spindles and isolated chromosomes (Fig. S4C,D). In summary, altering the XPB and Cdk7 functions in pre-MBT embryos causes defects in mitosis similar to those resulting from depleting XPD (Li et al., 2010) or p8 (this study).

Journal of Cell Science (2018) 131, jcs211631. doi:10.1242/jcs.211631

Therefore, deficiency of core and CAK TFIIH subunits in the early fly embryo catastrophically affects mitosis.

Misregulation of the expression of maternal transcripts caused by p8 depletion is correlated with the penetrance of mitotic defects in the early embryo

In addition to the fundamental activity of TFIIH in serine 5 phosphorylation of the CTD of RNAPII, TFIIH is also necessary for opening the DNA at the transcription initiation site (Kouzine et al., 2013; Alekseev et al., 2017). Therefore, although wild-type levels of RNAPIIS5P were observed in *p8*-null ovaries and early embryos (Fig. 4B,G), we were intrigued by the possibility that the mitotic phenotypes observed were caused by transcriptional defects during oogenesis or in pre-MBT stages. To determine the effect of the absence of p8 on global transcription, we performed RNA-seq analysis of individual *p8*-null ($p8^{-}/p8^{-}$) and *p8*-heterozygous ($p8^{+}/p8^{-}$) embryos, which show mitotic defects and wild-type phenotypes, respectively (Fig. 5A). Using this strategy, we could determine whether the mitotic defects in p8-depleted embryos were associated with the deregulation of maternal transcripts or the deregulation in genes expressed pre-MBT. *p8*-null or *p8*-heterozygous females expressing H2Av–RFP were used to collect embryos between NC9 and NC10. Then, total RNA from two heterozygous (Fig. 5A, embryos G and H) and three *p8*-null (Fig. 5A, embryos A, B and E) organisms were subjected to single-embryo transcriptome analyses by following the single-cell protocol for RNA-seq. These analyses showed genome map rates higher than 90% and identified nearly 8000 different transcripts per embryo and almost 4000 genes that were differentially regulated between the wild-type and the mutant embryos (Tables S1–S7).

The correlation analysis of the two control embryo (*p8* heterozygous) samples indicated similar levels of most of the detected transcripts; although, as expected, some variability was observed for the biological samples (Fig. 5B, embryo H versus embryo G). In contrast, comparison of the controls (embryos G or H) and *p8*-null embryos (embryos A, B and E) showed a large variation in the levels of many transcripts (Fig. 5B; Fig. S6). The *p8*-null embryos A and B clearly showed more severe mitotic phenotypes than embryo E, which showed less dramatic defects (Fig. 5A). Interestingly, the global gene expression in embryo E was

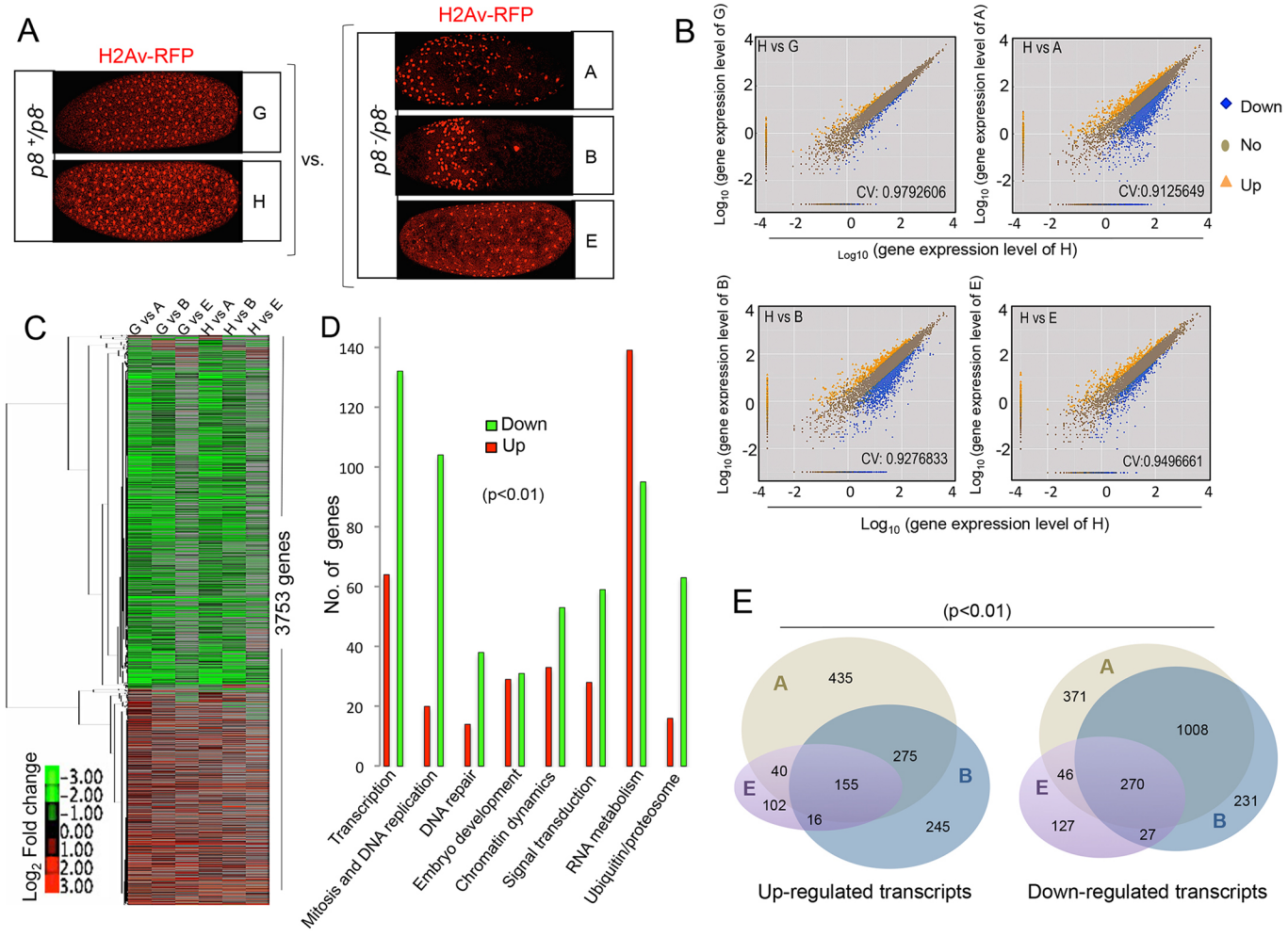

Fig. 5. Transcriptomic analysis of *p8*-null or *p8*-heterozygote embryos. (A) Heterozygous *p8*-null ($p8^{+}/p8^{-}$; *H2Av-RFP*/+) embryos (embryos G and H) and homozygous *p8*-null ($p8^{-}/p8^{-}$; *H2Av-RFP*/+) embryos, with defects in mitosis (embryos A, B and E) at division NC9 and NC10, used for single embryo RNA-seq analysis. (B) Correlation plots indicating the differences in gene expression between *p8*-null homozygous (A, B and E) and control (G and H) embryos. (C) Heat map showing the variations in gene expression between the two control embryos (G and H) and the three mutants (A, B and E). Note the low variation in embryo E compared with embryos A and B with more severe mutant phenotype. (D) Ontology analysis of affected genes identified by RNA-seq, whose function may be related to the catastrophic mitosis phenotype. (E) Venn diagrams that indicate the number of down- and upregulated genes affected in all the p8-depleted embryos.

Journal of Cell Science (2018) 131, jcs211631. doi:10.1242/jcs.211631

less affected (Fig. 5B,C), indicating a correlation between the severity of the mitotic defect phenotype and the degree of influence on global gene expression. We identified a group of 270 downregulated genes shared among all of our p8-depleted samples, suggesting that these genes are particularly sensitive to the transcriptional deregulation caused by the absence of p8 (Fig. 5E). The RNA-seq data showed that most of the deregulated transcripts in the *p8*-null embryos came from the maternal contribution (Table S7), suggesting aberrant transcription during oogenesis in *p8*-null females. In agreement with the *p8*-null embryo phenotypes, gene ontology analysis based on cellular functions that may be related to the observed phenotypes showed the downregulation of 104 genes encoding factors that participate in DNA replication or mitosis (Fig. 5D; Table S8). Intriguingly, 139 genes that participate in RNA metabolism are upregulated (Fig. 5D; Table S9). Taken together, these observations suggest that deregulated gene expression during oogenesis caused by mutations in TFIIH leads to catastrophic mitosis in early syncytial blastoderm embryos.

DISCUSSION

ZGA in the *Drosophila* embryo occurs in two waves, with the first involving the transcription of a small group of genes at the pre-MBT, and the second including the transcription of an important fraction of the zygotic genome at the MBT (Lee et al., 2014). At these stages, the dynamics of basal transcription machinery have been poorly studied. In *Drosophila*, only a few reports by our group and others on some TFIIH subunits (Aguilar-Fuentes et al., 2006; Li et al., 2013) and RNAPII and TATA-binding protein (TBP) dynamics (Seydoux and Dunn, 1997; Wang and Lindquist, 1998) exist. In this work, we have extended our analysis of the dynamics of TFIIH by immunostaining and *in vivo* studies using recombinant fluorescent proteins, and found that some subunits of TFIIH overlap with mitotic chromosomes during nuclear division cycles in pre-MBT embryos. In addition, we found that mutations in some TFIIH core subunits cause catastrophic mitosis during early embryonic development, at least partially resulting from the deregulation of global transcription during oogenesis.

Dynamic behaviour of TFIIH in *Drosophila* early syncytial blastoderm nuclear division cycles

Several studies have been performed to observe the subcellular and molecular dynamics of TFIIH during transcription, and the DNA damage response in cells during interphase (Giglia-Mari et al., 2006; Nonnekens et al., 2013). Nonetheless, the dynamics of TFIIH components throughout the cell cycle progression have been less extensively studied. Importantly, although a previous study showed the dynamics of the XPB core subunit *in vivo* in a mouse XPB–YFP knock-in model, that report focused on comparing the mobility of fluorescently tagged XPB in interphase cells that had the capacity to proliferate and in post-mitotic non-proliferative cells. By using FRAP, Giglia-Mari and colleagues showed that XPB mobility was lower in post-mitotic differentiated cells (Giglia-Mari et al., 2009). Thus, to our knowledge, our work is a pioneer study of the *in vivo* dynamics of TFIIH throughout the cell cycle progression in the context of the whole organism. Here, we showed that TFIIH is highly dynamic during fast nuclear division cycles in the early fly embryo. Our *in vivo* analyses showed that, although TFIIH overlaps with chromosomes, the intensity of the nuclear signal changed with cell cycle progression. During interphase, cytoplasmic localization was detected, but most of the TFIIH signal was observed in the nucleus. Interestingly, during chromatin condensation at prophase, the signal further increased inside the nucleus, while decreasing in the cytoplasm, suggesting translocation of TFIIH into the nucleus at this stage. Additionally, TFIIH foci were clearly observed at this stage, and these data suggest that some transcription at the pre-MBT occurs at this point.

We have demonstrated that TFIIH oscillated between the cytoplasm and the nucleus during cell cycle progression in pre-MBT embryos. A previous study described the localization of general transcription factors in HeLa cells during the transition from mitosis to G1. Unlike TBP, which was found on chromosomes throughout mitosis, other general transcription factors, including RNAPII, XPB and XPD, were localized in daughter nuclei only after mid-telophase (Prasanth et al., 2003). Hence, this intriguing behaviour observed for TFIIH in fly embryos could reflect a mechanism involved in the regulation of transcription during very short nuclear division cycles, such as those that occur at pre-MBT stages, where incomplete nuclear membrane breakdown occurs.

Importantly, the observation that the CycH and Cdk7 signals overlap with chromosomes during mitosis in wild-type embryos differs from a previous study suggesting that CAK is nuclear during interphase, but is excluded from mitotic chromosomes through an XPD-dependent mechanism. Specifically, in syncytial blastoderm embryos, XPD-depletion causes defects in mitosis and aberrant Cdk7 overlapping with chromosomes at anaphase (Li et al., 2010). Despite our efforts to analyse the Cdk7 localization pattern by immunostaining with several available antibodies, we could not observe clear nuclear signals during interphase in wild-type embryos. However, we did observe identical localization using the Cdk7–EGFP protein to that observed for other TFIIH subunits during replicative cycles in the syncytial blastoderm, including overlap between the CAK and mitotic chromosomes (Fig. S4; Movie 4). Thus, this discrepancy could be a consequence of the antibodies used to recognize Cdk7 not generating a good signal in embryonic immunostaining. Indeed, in agreement with our observations for other TFIIH subunits in pre-MBT embryos, Ito and colleagues reported that the XPD signal spreads in the nucleoplasm, but is enriched at the mitotic spindle at metaphase in human cells (Ito et al., 2010). Interestingly, an increasing number of studies have recently highlighted the existence of ‘mitotic bookmarking’ by several transcription factors (reviewed in Kadauke and Blobel, 2013). Our observations on TFIIH dynamics suggest that TFIIH might also be involved in bookmarking during early embryonic development, and this is currently under investigation.

TFIIH is maintained on mitotic chromosomes in the early fly embryo

An interesting feature of TFIIH dynamics is its enrichment in nuclear foci that overlap with active RNAPII foci that could correspond to HLBs. Transcriptional activation of the histone gene cluster during the pre-MBT in *Drosophila* has been well documented (Günesdogan et al., 2014). Except for histone H1, the transcription of histone genes depends on TATA box promoters and TBP binding. Indeed, HLBs are sites of TBP and RNAPII enrichment (Isogai et al., 2007; Guglielmi et al., 2013). Importantly, HLBs have been observed from interphase through metaphase (Isogai et al., 2007), as we also observed for TFIIH foci. As previously reported for HLBs (Salzler et al., 2013), TFIIH foci are maintained throughout the division cycle and disappear at late metaphase; a similar behaviour is observed for active RNAPII (Blythe and Wieschaus, 2016). Despite the generally accepted model of transcription being shut off in mitotic nuclei (Gottesfeld and Forbes, 1997), some transcription can reportedly occur during

Journal of Cell Science (2018) 131, jcs211631. doi:10.1242/jcs.211631

mitosis; for instance, transcription of the *CycB* gene in HeLa cells (Sciortino et al., 2001) and α-satellite DNA in centromeres (Chan et al., 2012). In the pre-MBT embryo, the time period for transcription is very short because the nuclear cycle has only a brief interphase and mostly consists of the S and M phases (Farrell and O'Farrell, 2014). Histone genes are transcribed during S phase (Guglielmi et al., 2013); however, for the pre-MBT stages, it is possible that transcription could be extended during the fast nuclear division cycle to achieve the amount of pre-MBT mRNA required during this developmental stage. The overlap of some TFIIH subunits with chromosomes in all nuclei division cycle stages in early embryos suggests a mechanism to retain some TFIIH for fast transcriptional re-activation after mitosis.

Early embryonic catastrophic mitosis and transcriptional defects caused by mutations in the TFIIH core and CAK subunits

Previous reports have suggested a role for the TFIIH XPD subunit in controlling Cdk7 functionality in cell cycle modulation during early fly embryogenesis (Chen et al., 2003; Li et al., 2010). In addition, XPD is a component of the MMXD complex involved in chromosome segregation in human cells (Ito et al., 2010). Furthermore, the ATPase activity of XPD is well known to be important for the formation of the open complex in RNAPII-transcribed genes, and it acts as a scaffold to maintain the integrity of TFIIH during transcription (Lainé et al., 2006; Kuper et al., 2014). Thus, further analyses to clarify the role of XPD in cell cycle regulation are required. Herein, we showed that mutations in the p8 and XPB core subunits of TFIIH, as well as the depletion of Cdk7, cause defects in mitosis, suggesting that this phenotype is not exclusive to the Cdk7 delocalization seen upon XPD depletion in fly embryos. In accordance, Matsuno and colleagues reported that mutations in p52, XPB and Cdk7 produced similar defects in cell cycle progression during fly eye imaginal disc development, suggesting that CAK activity in cell cycle regulation is performed by the holo-TFIIH complex (Matsuno et al., 2007). However, although a direct role for the holo-TFIIH complex in mitosis cannot be discarded, the evidence presented in this work indicates that the absence of p8 leads to deregulated gene expression during oogenesis, thus affecting the expression of many genes that participate in coordinated mitosis at the pre-blastoderm and syncytial blastoderm stages. On the other hand, our results that show the presence of the CAK subunits on mitotic chromosomes, challenging the model that proposes that only in the absence of XPD is Cdk7 maintained on the chromosomes during mitosis, causing catastrophic mitosis (Li et al., 2010).

Interestingly, embryos from females with decreased abundance of the transcriptional activator vielfältig/Zelda, which activates the onset of zygotic transcription, display mitotic defects with some similarities to those reported for XPD-deficient embryo phenotypes, and those observed here for *p8*-null, homozygous hay^{nc2} and Cdk7-depleted embryos (Staudt et al., 2006). It is thus difficult to distinguish between possible roles of TFIIH subunits in mitosis and indirect effects due to defective gene expression, particularly because some of the genes expressed at the pre-MBT stage may also participate in mitosis.

Despite the essential role for p8 in maintaining a steady-state level of cellular TFIIH proposed in human cells (Giglia-Mari et al., 2004), we did not observe a significant reduction in other TFIIH subunits in p8-depleted ovaries or embryos (this work) or in spermatogenesis (Cruz-Becerra et al., 2016). Furthermore, our transcriptome analyses of p8-depleted embryos highlight the importance of this protein in global transcription during development, as was recently observed in a p8-knockout mouse model, where absence of p8 caused embryonic lethality (Theil et al., 2013).

In conclusion, our analysis of TFIIH at the pre-MBT shows how this complex is distributed at chromosomes in waves during mitotic cycles, and that depletion of TFIIH subunits affects transcription during oogenesis and causes catastrophic mitosis in syncytial blastoderm embryos. This knowledge provides important insights into the functions of TFIIH during early embryonic development.

MATERIALS AND METHODS

Fly stocks

Oregon R was used as the wild-type strain, except when indicated. The *His2Av-RFP* transgenic lines (BL23650 and BL23651) and the GAL4 driver line (BL7063) were obtained from the Bloomington *Drosophila* Stock Center. The *Cdk7i* line (v10424) was obtained from the Vienna *Drosophila* Resource Center. The EYFP–p52, p8–ECFP and XPB–EGFP transgenic lines, as well as the *p8*-null and hay^{nc2} alleles were previously described (Cruz-Becerra et al., 2016; Herrera-Cruz et al., 2012; Regan and Fuller, 1988).

Transgenic flies

Recombinant DNA was generated by tagging the 5′ or 3′ end of the corresponding full-length cDNA coding sequence with the DNA sequence of the different fluorescent proteins used in this work. The recombinant DNA was cloned into the pCaSper-Hsp83 vector and used by BestGene Inc. to generate transgenic flies through standard microinjection protocols.

RNA interference assays

Line *v10442* (http://flybase.org/reports/FBsf0000074319.html) expressing a dsRNA against the *cdk7* transcript under the control of the *UAS-Gal4* system was crossed with the *P{matα4-GAL-VP16}* driver that expressed Gal4 from the *α-Tubulina67c* promoter in the ovaries. The resulting females flies with the genotype *v10442/+; P{matα4-GAL-VP16}/+* were crossed with wild-type males and the ovaries and the embryos analysed in western blot experiments and embryo immunostainings.

Immunostaining

Embryos were fixed in formaldehyde and heptane as previously described (Reynaud et al., 1999; Aguilar-Fuentes et al., 2006; Chen et al., 2013), except that methanol was used as fixative for tubulin staining. Immunostainings were performed by standard methods with the antibodies against p8 (1:100; Herrera-Cruz et al., 2012), $H_3S_{10}P$ (1:1500; cat. no SC-8656, Santa Cruz Biotechnology), AA4.3 (1:800; cat. no AB-579793, DSHB), ADL67.1 (1:600; cat. no AB-528336, DSHB), H14 (1:500; cat. no MMS-134-500, Covance), TBP (1:100; cat. no SC-273, Santa Cruz Biotechnology), CTD4H8 (1:100; cat. no SC-7495, Santa Cruz Biotechnology), GTU-88 (1:500; cat. no SC-11316, Abcam), CycH (1:500; cat. no SC-1662, Santa Cruz Biotechnology), and Alexa Fluor-conjugated secondary antibodies (Invitrogen). DNA was visualized by staining with either SYTOX Green (Invitrogen) or DAPI (Roche). To avoid flattening, the embryos were supported in handcrafted mounting chambers.

Live imaging

Embryos collected on apple juice plates were dechorionated with 50% bleach, extensively washed with water, placed on heptane glue-treated coverslips, immediately covered with Halocarbon oil 700 (Sigma) and analysed by confocal microscopy. Time-lapse movies from live embryos during at least two consecutive nuclear division cycles were acquired with an Olympus FV1000 confocal system coupled to an inverted microscope. Several embryos from at least two independent transgenic lines of each fluorescently labelled protein were analysed.

Western blot

Total protein extracts were analysed by immunoblotting with standard procedures. The following antibodies were used: 8WG16 (1:1500; cat. no

MMS-126R-500, Covance), H14 (1:1500; cat. no MMS-134-500, Covance), XPD (1:1500; our own preparation), XPB (1:2000; our own preparation), p52 (1:1500; Villicaña et al., 2013), p8 (1:1000; Herrera-Cruz et al., 2012), Cdk7 (1:1000; cat. no SC-7344, Santa Cruz Biotechnology), TBP (1:500; cat. no SC-273, Santa Cruz Biotechnology), E7 (1:2000; cat. no AB2315513, DSHB). Horseradish peroxidase (HRP)-coupled secondary antibodies (1:3500; Invitrogen) were used for chemiluminescence detection through Thermo Scientific Pierce ECL.

Single embryo RNA-seq and bioinformatic analysis

Homozygous or heterozygous *p8*-null females expressing the *His2Av-mRFP* transgene were used to collect embryos at nuclear division cycles 9–10. Briefly, dechorionated embryos were placed on a coverslip, covered with a drop of RNAse-free water, and immediately analysed under confocal microscopy. *Z*-stacks were acquired (total acquisition time was no longer than 1 min) and converted into an image stack to determine the number of nuclei (visualized through the His2Av–RFP signal) of each embryo. Total RNA from single embryos in nuclear division cycles 9–10 was extracted with TRIzol (Invitrogen), according to manufacturer's protocol. BGI performed RNA-seq analyses from single embryos. Briefly, mRNA enrichment was performed using oligo(dT). mRNA was fragmented and short fragments were used as template for the synthesis of cDNA by reverse transcription. Double-stranded cDNA was generated, purified and subjected to end repair and single nucleotide (adenine) addition. Adaptors were ligated and the libraries were amplified. The Agilent 2100 Bioanaylzer and ABI StepOnePlus Real-Time PCR System were used in quantification and qualification of the sample libraries. The libraries were sequenced using Illumina HiSeq™ 2000. Raw reads were filtered into clean reads aligned to the reference sequences. The alignment data was utilized to calculate the distribution of reads on reference genes and mapping ratio. The fragments per kilobase of transcript per million mapped reads (FPKM) method was used to calculate the expression levels. The correlation value between each two samples was calculated based on the FPKM result as recommended by the Encode plan in which the square of correlation value should be $\geq$0.92. The cluster analysis of gene expression patterns was performed by using cluster and java Treeview software. The details of the analysis are available upon request.

Acknowledgements

We thank Martha Vazquez and Viviana Valadez for discussions during the development of this work. We also thank Andres Saralegui, Arturo Pimentel and Chris Wood and the LNMA for advice in the use of the confocal microscopes.

Competing interests

The authors declare no competing or financial interests.

Author contributions

Conceptualization: G.C., M.Z.; Methodology: G.C., S.V.-C., M.J., A.B.-M.; Validation: G.C., M.Z.; Formal analysis: G.C., S.V.-C., M.Z.; Investigation: G.C., S.V.-C., M.J., A.B.-M.; Resources: M.Z.; Data curation: G.C., A.B.-M., M.Z.; Writing - original draft: G.C., M.Z.; Writing - review & editing: G.C., M.Z.; Supervision: M.Z.; Project administration: M.Z.; Funding acquisition: M.Z.

Funding

This work was supported by the Consejo Nacional de Ciencia y Tecnología (CONACyT) (grants 219673, 250588) and Programa de Apoyo a Proyectos de Investigación e Innovación Tecnológica (PAPIIT/UNAM) (grant IN200315) to M.Z.

Supplementary information

Supplementary information available online at
http://jcs.biologists.org/lookup/doi/10.1242/jcs.211631.supplemental

References

Abdulrahman, W., Iltis, I., Radu, L., Braun, C., Maglott-Roth, A., Giraudon, C., Egly, J.-M. and Poterszman, A. (2013). ARCH domain of XPD, an anchoring platform for CAK that conditions TFIIH DNA repair and transcription activities. *Proc. Natl. Acad. Sci. USA* **110**, E633-E642.

Aguilar-Fuentes, J., Valadez-Graham, V., Reynaud, E. and Zurita, M. (2006). TFIIH trafficking and its nuclear assembly during early *Drosophila* embryo development. *J. Cell Sci.* **119**, 3866-3875.

Alekseev, S., Nagy, Z., Sandoz, J., Weiss, A., Egly, J.-M., Le May, N. and Coin, F. (2017). Transcription without XPB establishes a unified helicase-independent mechanism of promoter opening in eukaryotic gene expression. *Mol. Cell* **65**, 504-514.

Ali-Murthy, Z., Lott, S. E., Eisen, M. B. and Kornberg, T. B. (2013). An essential role for zygotic expression in the pre-cellular *Drosophila* embryo. *PLoS Genet.* **9**, e1003428.

Blythe, S. A. and Wieschaus, E. F. (2016). Establishment and maintenance of heritable chromatin structure during early *Drosophila* embryogenesis. *eLife* **5**, e20148.

Chan, F. L., Marshall, O. J., Saffery, R., Kim, B. W., Earle, E., Choo, K. H. A. and Wong, L. H. (2012). Active transcription and essential role of RNA polymerase II at the centromere during mitosis. *Proc. Natl. Acad. Sci. USA* **109**, 1979-1984.

Chen, J., Larochelle, S., Li, X. and Suter, B. (2003). Xpd/Ercc2 regulates CAK activity and mitotic progression. *Nature* **424**, 228-232.

Chen, K., Johnston, J., Shao, W., Meier, S., Staber, C. and Zeitlinger, J. (2013). A global change in RNA polymerase II pausing during the *Drosophila* midblastula transition. *eLife* **2**, e00861.

Coin, F., Oksenych, V. and Egly, J.-M. (2007). Distinct roles for the XPB/p52 and XPD/p44 subcomplexes of TFIIH in damaged DNA opening during nucleotide excision repair. *Mol. Cell* **26**, 245-256.

Compe, E. and Egly, J.-M. (2012). TFIIH: when transcription met DNA repair. *Nat. Rev. Mol. Cell. Biol.* **13**, 343-354.

Cruz-Becerra, G., Juárez, M., Valadez-Graham, V. and Zurita, M. (2016). Analysis of *Drosophila* p8 and p52 mutants reveals distinct roles for the maintenance of TFIIH stability and male germ cell differentiation. *Open Biol.* **6**, 160222.

De Renzis, S., Elemento, O., Tavazoie, S. and Wieschaus, E. F. (2007). Unmasking activation of the zygotic genome using chromosomal deletions in the *Drosophila* embryo. *PLoS Biol.* **25**, e117.

Egly, J.-M. and Coin, F. (2011). A history of TFIIH: two decades of molecular biology on a pivotal transcription/repair factor. *DNA Repair* **10**, 714-721.

Farrell, J. A. and O'Farrell, P. H. (2014). From egg to gastrula: how the cell cycle is remodeled during the *Drosophila* mid-blastula transition. *Annu. Rev. Genet.* **48**, 269-294.

Fishburn, J., Tomko, E., Galburt, E. and Hahn, S. (2015). Double-stranded DNA translocase activity of transcription factor TFIIH and the mechanism of RNA polymerase II open complex formation. *Proc. Natl. Acad. Sci. USA* **112**, 3961-3966.

Foe, V. E. and Alberts, B. M. (1983). Studies of nuclear and cytoplasmic behaviour during the five mitotic cycles that precede gastrulation in *Drosophila* embryogenesis. *J. Cell Sci.* **61**, 31-70.

Fregoso, M., Lainé, J.-P., Aguilar-Fuentes, J., Mocquet, V., Reynaud, E., Coin, F., Egly, J.-M. and Zurita, M. (2007). DNA repair and transcriptional deficiencies caused by mutations in the *Drosophila* p52 subunit of TFIIH generate developmental defects and chromosome fragility. *Mol. Cell. Biol.* **27**, 3640-3650.

Giglia-Mari, G., Coin, F., Ranish, J. A., Hoogstraten, D., Theil, A., Wijgers, N., Jaspers, N. G. J., Raams, A., Argentini, M., van der Spek, P. J. et al. (2004). A new, tenth subunit of TFIIH is responsible for the DNA repair syndrome trichothiodystrophy group A. *Nat. Genet.* **36**, 714-719.

Giglia-Mari, G., Miquel, C., Theil, A. F., Mari, P.-O., Hoogstraten, D., Ng, J. M. Y., Dinant, C., Hoeijmakers, J. H. J. and Vermeulen, W. (2006). Dynamic interaction of TTDA with TFIIH is stabilized by nucleotide excision repair in living cells. *PLoS Biol.* **4**, e156.

Giglia-Mari, G., Theil, A. F., Mari, P.-O., Mourgues, S., Nonnekens, J., Andrieux, L. O., de Wit, J., Miquel, C., Wijgers, N., Maas, A. et al. (2009). Differentiation driven changes in the dynamic organization of Basal transcription initiation. *PLoS Biol.* **7**, e1000220.

Gottesfeld, J. M. and Forbes, D. J. (1997). Mitotic repression of the transcriptional machinery. *Trends Biochem. Sci.* **22**, 197-202.

Guglielmi, B., La Rochelle, N. and Tjian, R. (2013). Gene-specific transcriptional mechanisms at the histone gene cluster revealed by single-cell imaging. *Mol. Cell* **51**, 480-492.

Günesdogan, U., Jäckle, H. and Herzig, A. (2014). Histone supply regulates S phase timing and cell cycle progression. *eLife* **3**, e02443.

Harel, A., Zlotkin, E., Nainudel-Epszteyn, S., Feinstein, N., Fisher, P. A. and Gruenbaum, Y. (1989). Persistence of major nuclear envelope antigens in an envelope-like structure during mitosis in *Drosophila melanogaster* embryos. *J. Cell Sci.* **94**, 463-470.

Herrera-Cruz, M., Cruz, G., Valadez-Graham, V., Fregoso-Lomas, M., Villicaña, C., Vázquez, M., Reynaud, E. and Zurita, M. (2012). Physical and functional interactions between *Drosophila* homologue of Swc6/p18Hamlet subunit of the SWR1/SRCAP chromatin-remodeling complex with the DNA repair/transcription factor TFIIH. *J. Biol. Chem.* **287**, 33567-33580.

Hsin, J.-P. and Manley, J. L. (2012). The RNA polymerase II CTD coordinates transcription and RNA processing. *Genes Dev.* **26**, 2119-2137.

Isogai, Y., Keles, S., Prestel, M., Hochheimer, A. and Tjian, R. (2007). Transcription of histone gene cluster by differential core-promoter factors. *Genes Dev.* **21**, 2936-2949.

Ito, S., Tan, L. J., Andoh, D., Narita, T., Seki, M., Hirano, Y., Narita, K., Kuraoka, I., Hiraoka, Y. and Tanaka, K. (2010). MMXD, a TFIIH-independent XPD-MMS19 protein complex involved in chromosome segregation. *Mol. Cell* **39**, 632-640.

Jawhari, A., Lainé, J.-P., Dubaele, S., Lamour, V., Poterszman, A., Coin, F., Moras, D. and Egly, J.-M. (2002). p52 Mediates XPB function within the transcription/repair factor TFIIH. *J. Biol. Chem.* **277**, 31761-31767.
Kadauke, S. and Blobel, G. A. (2013). Mitotic bookmarking by transcription factors. *Epigenet. Chromatin.* **6**, 6.
Kainov, D. E., Vitorino, M., Cavarelli, J., Poterszman, A. and Egly, J.-M. (2008). Structural basis for group A trichothiodystrophy. *Nat. Struct. Mol. Biol.* **15**, 980-984.
Kouzine, F., Wojtowicz, D., Yamane, A., Resch, W., Kieffer-Kwon, K.-R., Bandle, R., Nelson, S., Nakahashi, H., Awasthi, P., Feigenbaum, L. et al. (2013). Global regulation of promoter melting in naive lymphocytes. *Cell* **153**, 988-999.
Kuper, J., Braun, C., Elias, A., Michels, G., Sauer, F., Schmitt, D. R., Poterszman, A., Egly, J.-M. and Kisker, C. (2014). In TFIIH, XPD helicase is exclusively devoted to DNA repair. *PLoS Biol.* **12**, e1001954.
Lainé, J. P., Mocquet, V. and Egly, J. M. (2006). TFIIH enzymatic activities in transcription and nucleotide excision repair. *Methods Enzymol.* **408**, 246-263.
Larochelle, S., Merrick, K. A., Terret, M.-E., Wohlbold, L., Barboza, N. M., Zhang, C., Shokat, K. M., Jallepalli, P. V. and Fisher, R. P. (2007). Requirements for Cdk7 in the assembly of Cdk1/cyclin B and activation of Cdk2 revealed by chemical genetics in human cells. *Mol. Cell* **25**, 839-850.
Lee, M. T., Bonneau, A. R. and Giraldez, A. J. (2014). Zygotic genome activation during the maternal-to-zygotic transition. *Annu. Rev. Cell Dev. Biol.* **30**, 581-613.
Li, X., Urwyler, O. and Suter, B. (2010). *Drosophila* Xpd regulates Cdk7 localization, mitotic kinase activity, spindle dynamics, and chromosome segregation. *PLoS Genet.* **6**, e1000876.
Li, X.-Y., Harrison, M. M., Villalta, J. E., Kaplan, T. and Eisen, M. B. (2014). Establishment of regions of genomic activity during the *Drosophila* maternal to zygotic transition. *eLife* **3**, e03737.
Lott, S. E., Villalta, J. E., Schroth, G. P., Luo, S., Tonkin, L. A. and Eisen, M. B. (2011). Noncanonical compensation of zygotic X transcription in early *Drosophila* melanogaster development revealed through single-embryo RNA-seq. *PLoS Biol.* **9**, e1000590.
Matsuno, M., Kose, H., Okabe, M. and Hiromi, Y. (2007). TFIIH controls developmentally-regulated cell cycle progression as a holocomplex. *Genes Cells* **12**, 1289-1300.
Mazumdar, A. and Mazumdar, M. (2002). How one becomes many: blastoderm cellularization in *Drosophila melanogaster*. *BioEssays* **24**, 1012-1022.
Merino, C., Reynaud, E., Vázquez, M. and Zurita, M. (2002). DNA repair and transcriptional effects of mutations in TFIIH in *Drosophila* development. *Mol. Biol. Cell* **13**, 3246-3256.
Mounkes, L. C., Jones, R. S., Liang, B.-C., Gelbart, W. and Fuller, M. T. (1992). A *Drosophila* model for xeroderma pigmentosum and Cockayne's syndrome: haywire encodes the fly homolog of ERCC3, a human excision repair gene. *Cell* **71**, 925-937.
Nizami, Z. F., Deryusheva, S. and Gall, J. G. (2010). Cajal bodies and histone locus bodies in *Drosophila* and *Xenopus*. *Cold Spring Harb. Symp. Quant. Biol.* **75**, 313-320.
Nonnekens, J., Cabantous, S., Slingerland, J., Mari, P.-O. and Giglia-Mari, G. (2013). In vivo interactions of TTDA mutant proteins within TFIIH. *J. Cell Sci.* **126**, 3278-3283.
Prasanth, K. V., Sacco-Bubulya, P. A., Prasanth, S. G. and Spector, D. L. (2003). Sequential entry of components of gene expression machinery into daughter nuclei. *Mol. Biol. Cell* **14**, 1043-1057.
Pritchard, D. K. and Schubiger, G. (1996). Activation of transcription in Drosophila embryos is a gradual process mediated by the nucleocytoplasmic ratio. *Genes Dev.* **10**, 1131-1142.
Regan, C. L. and Fuller, M. T. (1988). Interacting genes that affect microtubule function: the nc2 allele of the haywire locus fails to complement mutations in the testis-specific beta-tubulin gene of *Drosophila*. *Genes Dev.* **2**, 82-92.
Reynaud, E., Lomelí, H., Vázquez, M. and Zurita, M. (1999). The *Drosophila* melanogaster homologue of the Xeroderma pigmentosum D gene product is located in euchromatic regions and has a dynamic response to UV light-induced lesions in polytene chromosomes. *Mol. Biol. Cell* **10**, 1191-1203.
Salzler, H. R., Tatomer, D. C., Malek, P. Y., McDaniel, S. L., Orlando, A. N., Marzluff, W. F. and Duronio, R. J. (2013). A sequence in the *Drosophila* H3-H4 Promoter triggers histone locus body assembly and biosynthesis of replication-coupled histone mRNAs. *Dev. Cell* **24**, 623-634.
Satija, R. and Bradley, R. K. (2012). The TAGteam motif facilitates binding of 21 sequence-specific transcription factors in the *Drosophila* embryo. *Genome Res.* **22**, 656-665.
Schachter, M. M. and Fisher, R. P. (2013). The CDK-activating kinase Cdk7: taking yes for an answer. *Cell Cycle* **12**, 3239-3240.
Schuh, M., Lehner, C. F. and Heidmann, S. (2007). Incorporation of *Drosophila* CID/CENP-A and CENP-C into centromeres during early embryonic anaphase. *Curr. Biol.* **17**, 237-243.
Sciortino, S., Gurtner, A., Manni, I., Fontemaggi, G., Dey, A., Sacchi, A., Ozato, K. and Piaggio, G. (2001). The cyclin B1 gene is actively transcribed during mitosis in HeLa cells. *EMBO Rep.* **2**, 1018-1023.
Seydoux, G. and Dunn, M. A. (1997). Transcriptionally repressed germ cells lack a subpopulation of phosphorylated RNA polymerase II in early embryos of *Caenorhabditis elegans* and *Drosophila melanogaster*. *Development* **124**, 2191-2201.
Staudt, N., Fellert, S., Chung, H. R., Jäckle, H. and Vorbrüggen, G. (2006). Mutations of the *Drosophila* zinc finger-encoding gene vielfältig impair mitotic cell divisions and cause improper chromosome segregation. *Mol. Biol. Cell* **17**, 2356-2365.
Theil, A. F., Nonnekens, J., Steurer, B., Mari, P.-O., de Wit, J., Lemaitre, C., Marteijn, J. A., Raams, A., Maas, A., Vermeij, M. et al. (2013). Disruption of TTDA results in complete nucleotide excision repair deficiency and embryonic lethality. *PLoS Genet.* **9**, e1003431.
Villicaña, C., Cruz, G. and Zurita, M. (2013). The genetic depletion or the triptolide inhibition of TFIIH in p53-deficient cells induces a JNK-dependent cell death in *Drosophila*. *J. Cell Sci.* **126**, 2502-2515.
Wang, Z. and Lindquist, S. (1998). Developmentally regulated nuclear transport of transcription factors in *Drosophila* embryos enable the heat shock response. *Development* **125**, 4841-4850.
Yeom, E., Hong, S.-T. and Cho, K.-W. (2014). Crumbs interacts with Xpd for nuclear division control in *Drosophila*. *Oncogene* **34**, 2777-2789.
Zurita, M. and Merino, C. (2003). The transcriptional complexity of the TFIIH Complex. *Trends Genet.* **10**, 578-584.
Zurita, M., Reynaud, E. and Aguilar-Fuentes, J. (2008). From the beginning: the basal transcription machinery and onset of transcription in the early animal embryo. *Cell. Mol. Life Sci.* **65**, 212-227.

Supp. Fig 1

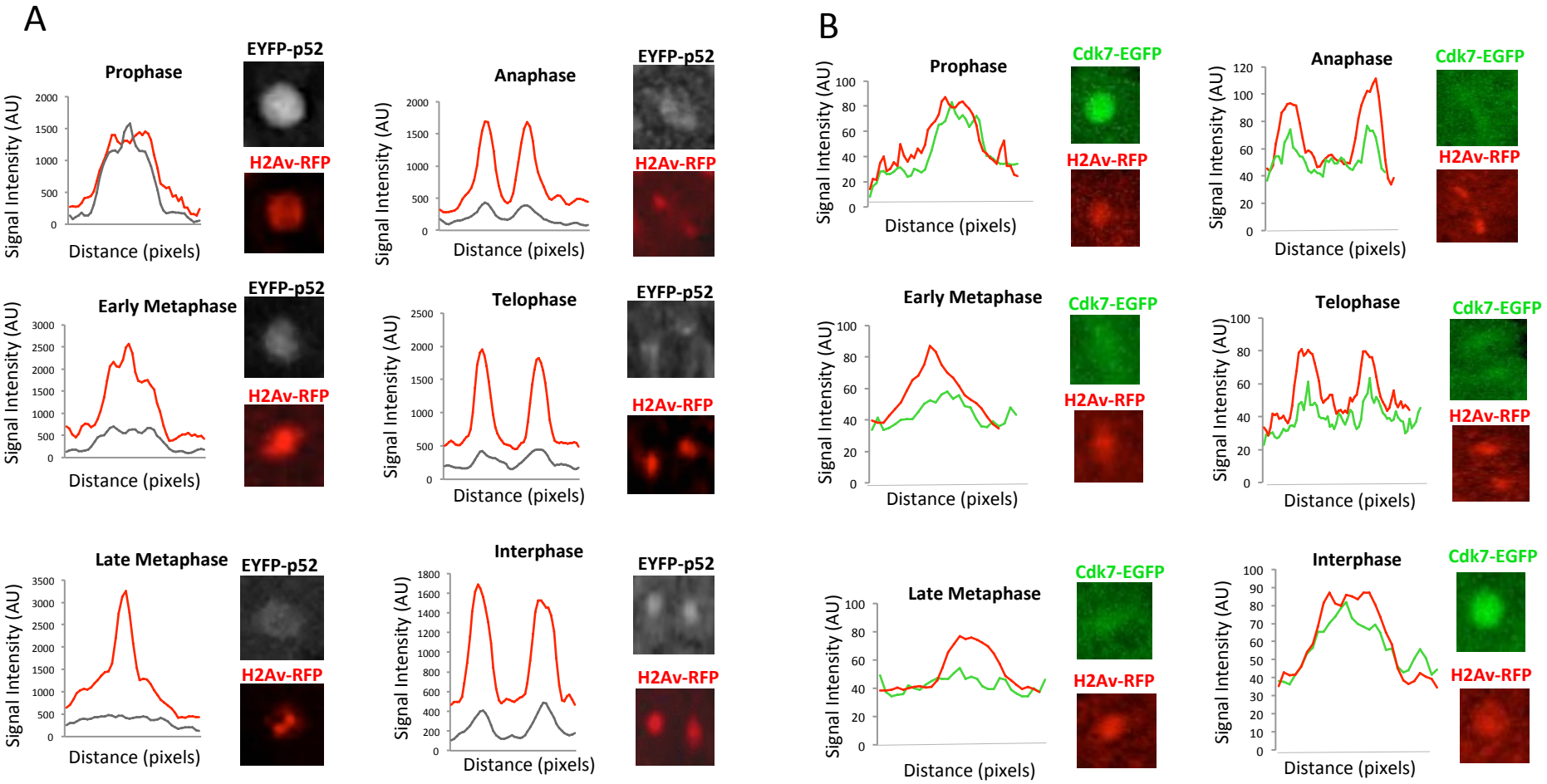

Supp. Fig. 1. **Oscillatory behaviour of TFIIH during a replicative cycle**. The images show the dynamics of EYFP-p52 (grey; panel A) and Cdk7-EGFP (green; panel B) during a replicative cycle. H2Av-RFP signal (red) was used as reference to visualize the chromatin state. The plots represent the signal intensity for each channel at the same plane.

Supp. Fig. 2

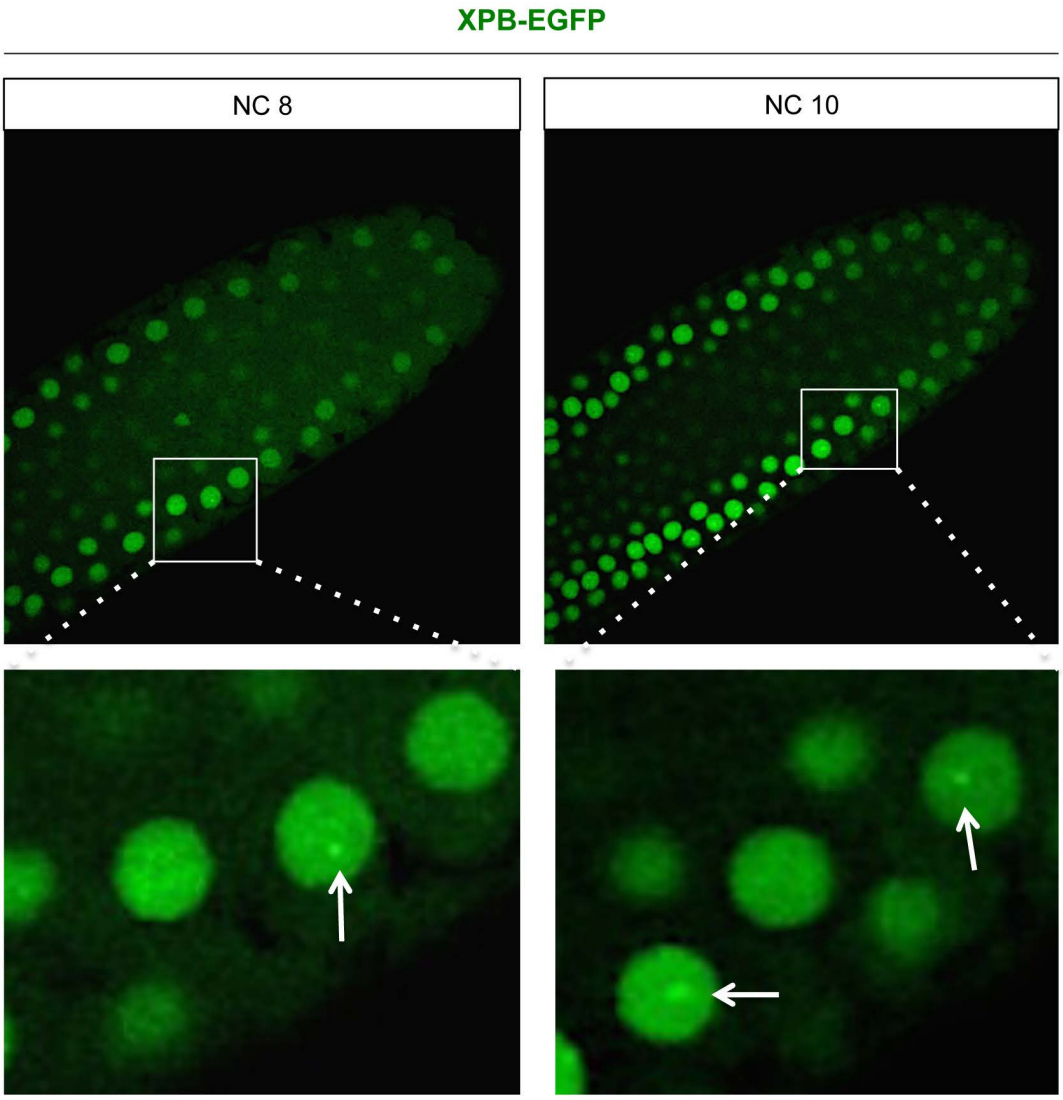

Supp. Fig. 2. **Visualization of XPB-EGFP in embryos at nuclear cycles (NC) 8 and 10.** XPB foci are indicated by arrows.

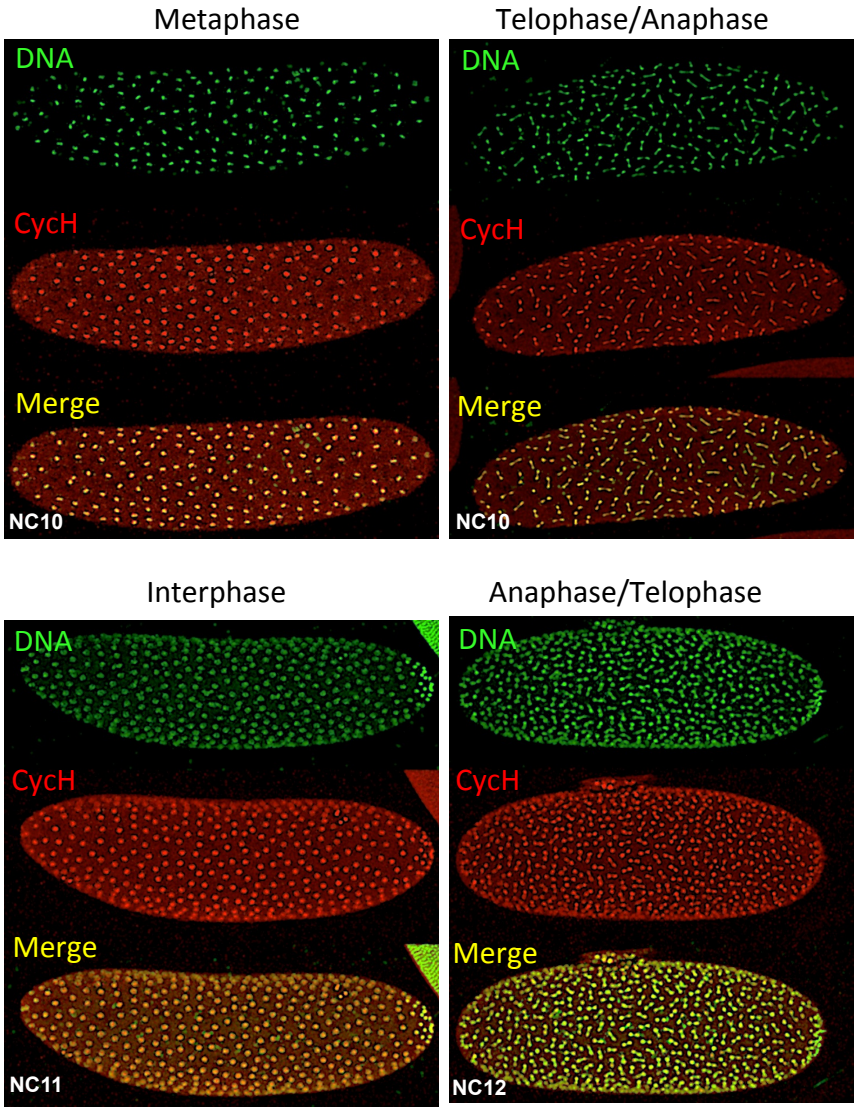

Supp. Fig. 3**. Detection of CycH by immunostaining in pre-MBT embryos**
The phases of the mitotic cycle are indicated. CycH signal is in red; DNA is in green.

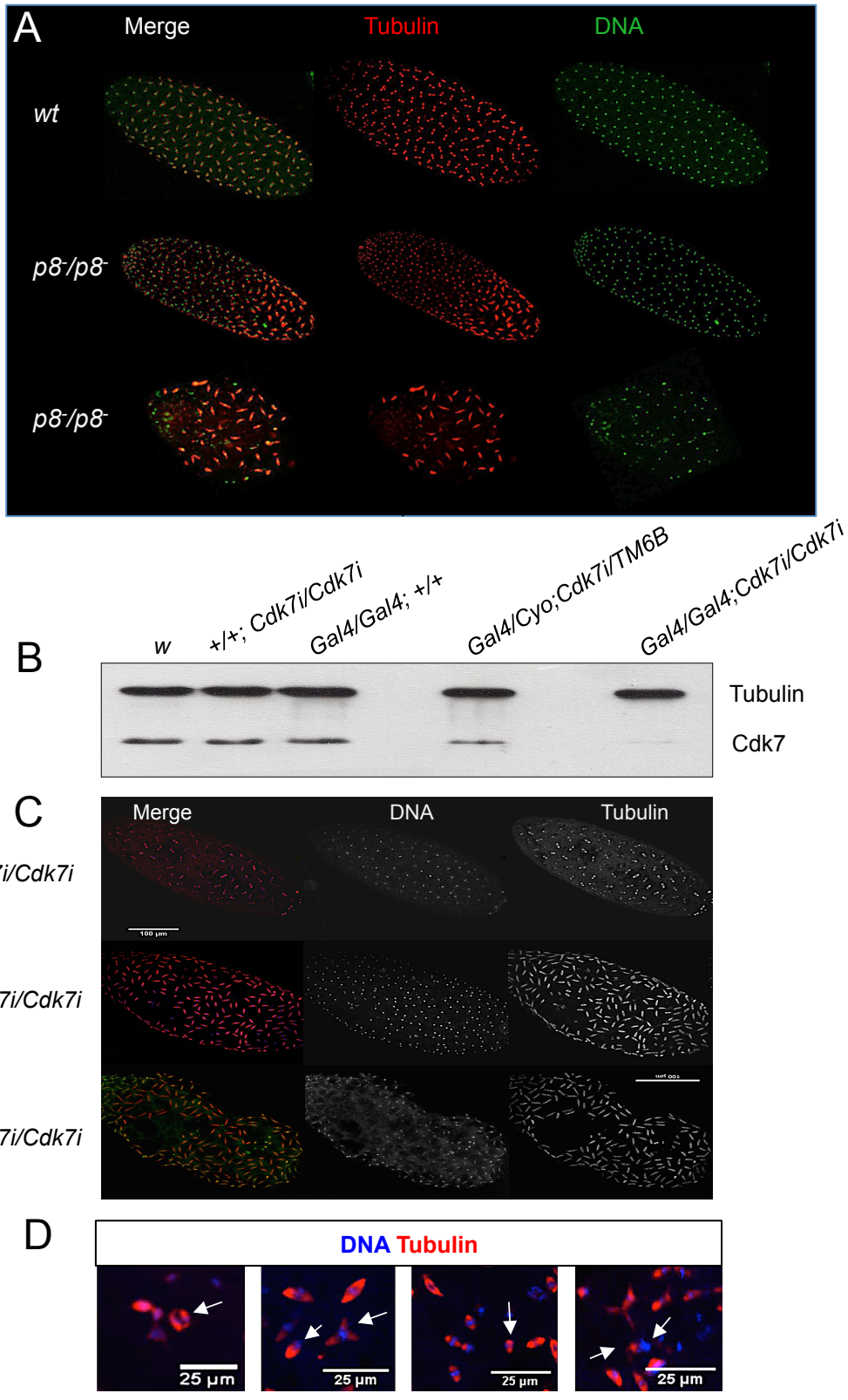

Supp. Fig. 4**. Syncytial blastoderm embryos deficient in p8 and Cdk7 have catastrophic mitosis.**
(A) The panel shows two embryos with low (middle panel) and severe (bottom panel) *p8* mutant phenotypes. DNA and alpha-tubulin staining are in green and red respectively.
(B) Western blot showing the reduction of Cdk7 protein in embryos from mothers that express an RNAi against Cdk7 (Cdk7i) during oogenesis.
(C) Example of mitotic defects in embryos depleted for Cdk7 showing different mitotic defects. The mother's genotypes are indicated. Aberrant spindles, and isolated chromosomes among other mitotic defects are indicated with arrows.
(D) Zoom of different mitotic defects observed in embryos with maternally depleted Cdk7.

Journal of Cell Science • Supplementary information

Supp. Fig. 6

A

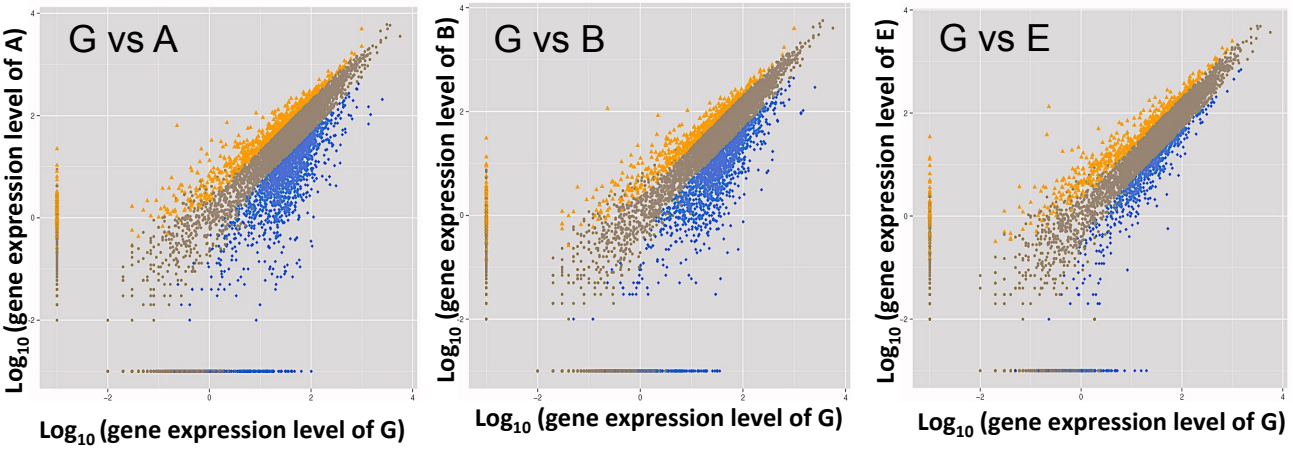

B

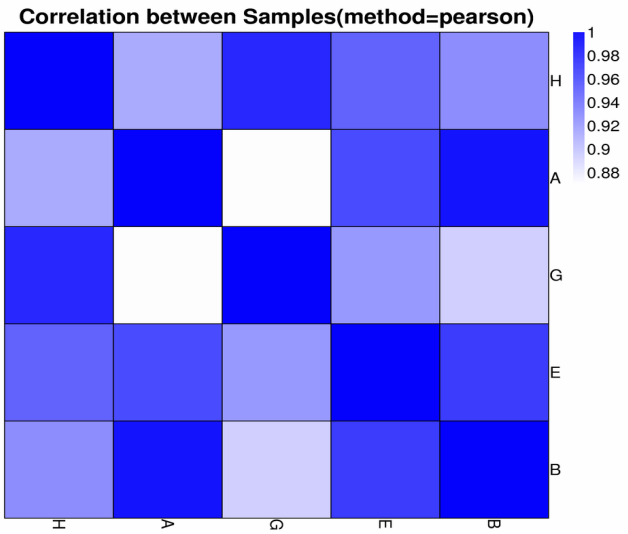

Supp. Fig. 5. **Correlation values of the transcriptome between a wild type embryo (G) and mutant embryos (A, B, and E) .**

A) Correlation plots between mutant embryos (A,B and E) and the wild type embryo G.

B) RNA-seq correlation values between the different embryos analysed.

Supplementary Movies

Supp. Movie 1. **In vivo dynamics of p52 in the syncytial blastoderm embryo.**
The movie shows EYFP-p52 (yellow) and H2Av-RFP (red). Note the presence of p52 foci during the nuclear cycles.

Supp. Movie 2. **In vivo dynamics of p52 (EYFP) and p8 (ECFP) in the syncytial blastoderm embryo.**

Supp. Movie 3**. In vivo dynamics of XPB.** The movie shows the dynamics of the XPB-EGFP recombinant protein in the syncytial blastoderm embryo.

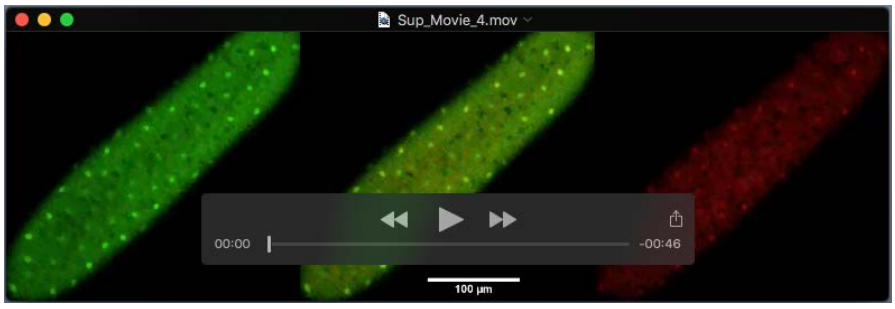

Supp. Movie 4. **In vivo dynamics of Cdk7**. The movie shows the dynamics of Cdk7-EGFP (green) and H2Av-RFP (red) in a syncytial blastoderm embryo.

Supplementary Tables

Supp. Table 1. Embryo G vs embryo A, Gene Diff. Expression

Click here to Download Table S1

Supp. Table 2. Embryo G vs embryo B, Gene Diff. Expression

Click here to Download Table S2

Supp. Table 3. Embryo G vs Embryo E, Gene Diff. Expression

Click here to Download Table S3

Supp. Table 4. Embryo H vs Embryo A, Gene Diff. Expression

Click here to Download Table S4

Supp. Table 5. Embryo H vs Embryo B, Gene Diff. Expression

Click here to Download Table S5

Supp. Table 6. Embryo H vs. Embryo E, Gene Diff. Expression

Click here to Download Table S6

Supp. Table 7. Total Filter.

Click here to Download Table S7

Supp. Table 8. Ontology, down regulated genes

Click here to Download Table S8

Supp. Table 9. Ontology, up regulated genes

Click here to Download Table S9